Chapter 1

Nuclear Fission II

"Thermal neutrons fission ^{235}U *because the compound nucleus is born above the barrier;* ^{238}U *needs fast neutrons because it is born below."*

standard reactor-physics summary [6, 1]

The preceding lecture, *Nuclear Fission I*, established that heavy nuclei have $Q > 0$ for fission yet are protected by a barrier of several MeV. This chapter applies that picture to neutron-induced fission of uranium: why thermal neutrons fission ^{235}U but not ^{238}U, what the mass-yield curve looks like, how asymmetry reduces Q relative to the symmetric maximum, why prompt and delayed neutrons appear, how the fission energy is partitioned, and how a chain reaction can be sustained [6, 1, 14, 2].

1.1 Neutron capture on ^{235}U: fissile behaviour

Natural uranium is mostly ^{238}U ($\sim 99.3\%$) with ^{235}U ($\sim 0.7\%$). Thermal-neutron fission of the latter is the workhorse of many reactors. The capture reaction is

$$^{235}\mathrm{U} + n \;\rightarrow\; ^{236}\mathrm{U}^* \;\rightarrow\; \text{fission fragments} + \text{neutrons}. \tag{1.1}$$

The capture Q-value (excitation energy deposited in ^{236}U when the neutron has negligible kinetic energy) is

$$Q = [m_n + M(^{235}\mathrm{U}) - M(^{236}\mathrm{U})]c^2 \approx 6.545\,\mathrm{MeV}. \tag{1.2}$$

Thus thermal capture forms $^{236}\mathrm{U}^*$ at about 6.55 MeV above its ground state.

An illustrative one-barrier estimate for ^{236}U is

$$E_f(^{236}\mathrm{U}) \sim 6\,\mathrm{MeV}. \tag{1.3}$$

Using $E_f \simeq 6.2\,\mathrm{MeV}$ for orientation,

$$Q \approx 6.55\,\mathrm{MeV} \;>\; E_f \approx 6.2\,\mathrm{MeV}, \tag{1.4}$$

the compound nucleus is formed above the representative saddle scale. Real actinide barriers are double-humped and depend on spin, parity, and excitation; barrier transmission and compound-nuclear resonances therefore remain part of the measured cross section even when this simple energy comparison is favourable. The thermal-neutron fission cross section is nevertheless large (hundreds of barns). Materials that fission with thermal neutrons are called **fissile**; examples are ^{235}U, ^{239}Pu, and ^{233}U [6, 1, 2].

Key idea

Thermal $n + {}^{235}\mathrm{U} \to {}^{236}\mathrm{U}^*$: $S_n \sim 6.55\,\mathrm{MeV}$ exceeds a representative $E_f \sim 6.2\,\mathrm{MeV}$. This explains why ^{235}U is fissile, but a double-humped transmission calculation replaces the one-barrier picture in quantitative work.

1.1.1 Competing channels

Not every neutron that meets ^{235}U causes fission. Important competitors include:

(i) **Elastic scattering:** $n + {}^{235}\mathrm{U} \to n' + {}^{235}\mathrm{U}$.

(ii) **Radiative capture:** $n + {}^{235}\mathrm{U} \to {}^{236}\mathrm{U}^* \to {}^{236}\mathrm{U} + \gamma$. If enough γ energy is radiated before fission, the excitation drops below E_f and fission becomes improbable. Ground-state ^{236}U then lives for α decay with a multi-million-year half-life.

The branching between fission and (n, γ) is encoded in the fission cross section σ_f and the capture cross section σ_γ [6, 1].

1.2 Neutron capture on ^{238}U: fertile behaviour

For ^{238}U,

$$^{238}\mathrm{U} + n \ \to \ ^{239}\mathrm{U}^*, \tag{1.5}$$

with capture Q-value

$$Q = [m_n + M(^{238}\mathrm{U}) - M(^{239}\mathrm{U})]c^2 \approx 4.806\,\mathrm{MeV}. \tag{1.6}$$

The effective fission barrier of ^{239}U is model-dependent and double-humped, but is of order 6 MeV. Using the 6.2 MeV one-barrier value adopted in the original lecture gives

$$Q \approx 4.806\,\mathrm{MeV} \ < \ E_f \approx 6.2\,\mathrm{MeV} : \tag{1.7}$$

thermal capture leaves the compound nucleus *below* the barrier. Fission requires tunneling through a residual barrier of order 1.4 MeV, so the thermal fission cross section is negligible.

If the neutron brings kinetic energy K_n, the excitation of $^{239}\mathrm{U}^*$ is approximately $Q + K_n$ (neglecting the small centre-of-mass correction). Fission becomes probable when

$$Q + K_n \gtrsim E_f \quad \Rightarrow \quad K_n \gtrsim E_f - Q \sim 1.4\,\mathrm{MeV}. \tag{1.8}$$

In practice a threshold near 1 MeV is observed: fast neutrons can fission ^{238}U, thermal neutrons cannot. ^{238}U is therefore called **fissionable** (by fast neutrons) but not fissile; it is also **fertile** because successive captures and β decays can breed ^{239}Pu [6, 1, 14].

Remark

The capture Q-values are neutron separation energies of the compound nuclei:

$$Q[n + {}^{235}\mathrm{U}] = S_n({}^{236}\mathrm{U}), \qquad Q[n + {}^{238}\mathrm{U}] = S_n({}^{239}\mathrm{U}).$$

The quoted 6.545 and 4.806 MeV values follow AME2020 masses (NNDC QCalc) [27, 21]. Barrier values are less sharply defined than masses because an actinide has inner and outer saddles; therefore $E_f - Q$ is an explanatory scale, not a precision prediction of the measured threshold.

Caution

The difference between ^{235}U and ^{238}U is not a gross difference in barrier height; both compound barriers are ~ 6 MeV. The decisive quantity is the neutron separation energy (capture Q) of the compound system: pairing makes even–even ^{236}U more tightly bound relative to $^{235}\mathrm{U} + n$ than odd ^{239}U is relative to $^{238}\mathrm{U} + n$.

Remark

Odd-A actinide targets (^{235}U, ^{239}Pu, ^{233}U) typically have larger capture Q values into even–even compound nuclei and are fissile. Even–even targets more often require fast neutrons [6, 1].

1.3 Fission fragment yields: asymmetric mass distribution

Once $^{236}\mathrm{U}^*$ is above the barrier, it does not split into a unique pair of fragments. Many partitions are open. Representative channels include

$$^{236}\mathrm{U} \to {}^{140}\mathrm{Xe} + {}^{94}\mathrm{Sr} + 2n, \tag{1.9}$$

$$^{236}\mathrm{U} \to {}^{139}\mathrm{Ba} + {}^{94}\mathrm{Kr} + 3n, \tag{1.10}$$

$$^{236}\mathrm{U} \to {}^{141}\mathrm{Cs} + {}^{93}\mathrm{Rb} + 2n, \tag{1.11}$$

$$^{236}\mathrm{U} \to {}^{137}\mathrm{I} + {}^{97}\mathrm{Y} + 2n. \tag{1.12}$$

Plotting the percentage yield against fragment mass number A produces the famous **double-humped mass-yield curve**: peaks near $A \sim 95$ and $A \sim 140$, with a deep valley at symmetric split $A \sim 118$. Symmetric fission is suppressed by roughly two orders of magnitude relative to the asymmetric peaks for thermal fission of ^{235}U, with the precise peak and valley values depending on whether independent, cumulative, or chain yields are plotted [6, 1, 2].

The pure liquid drop, with only surface and Coulomb energies, tends to favour symmetric scission near the barrier. The observed asymmetry is a **shell-structure** effect: fragments near closed shells (notably near $A \sim 132$, related to the doubly magic ^{132}Sn region) are preferentially formed. Liquid-drop theory remains excellent for the overall energetics and the existence of a barrier; it is incomplete for fine details of the yield curve [6, 14].

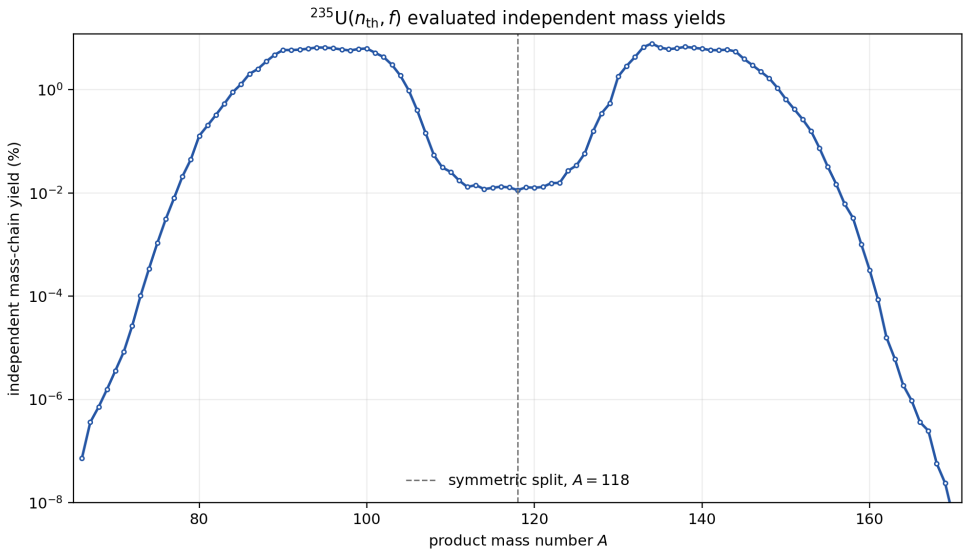

Figure 1.1: Independent mass-chain yields for thermal-neutron fission of ^{235}U, obtained by summing the ENDF/B-VIII.0 independent nuclide yields at fixed mass number A. The logarithmic ordinate faithfully displays both asymmetric peaks and the strongly suppressed symmetric region; the summed chain yield is two products per fission [35].

1.4 Energy release: B/A curve and asymmetry

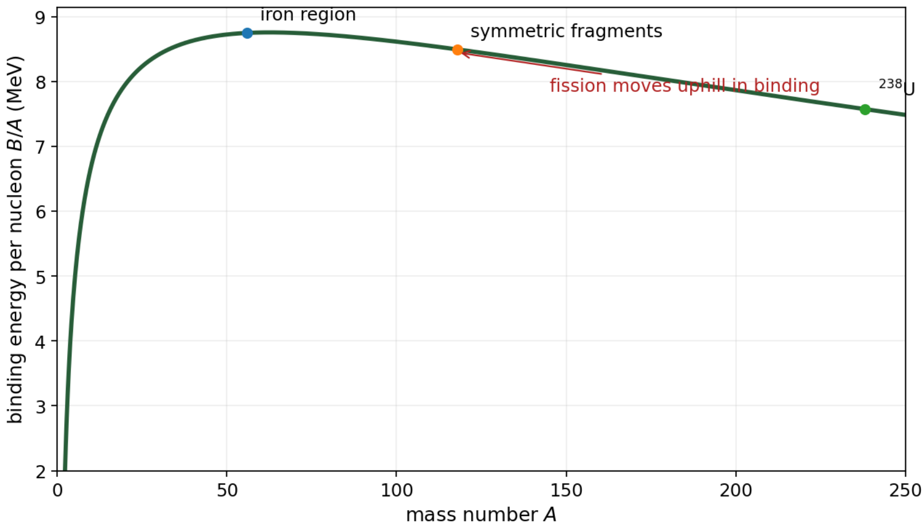

Figure 1.2: Binding energy per nucleon versus mass number. Heavy nuclei sit on the right-hand declining slope; fission products move toward the iron-peak region of higher B/A. Clean redraw of the curve on the original PH5001 Lecture 25 source page, checked against AME binding-energy systematics; the plotted curve is pedagogical rather than a mass evaluation.

Let the parent have mass number A and total binding $B_{\rm p}$. Write the fragments as

$$A_1 = \frac{A}{2} - a, \qquad A_2 = \frac{A}{2} + a, \tag{1.13}$$

where a measures mass asymmetry and neutron emission is temporarily suppressed. Let

$F(x) = x\,b(x)$ be the total binding of a representative fragment of mass x, with $b = B/A$. Then

$$Q(a) = F(A/2 - a) + F(A/2 + a) - B_{\mathrm{p}}. \tag{1.14}$$

Interchanging the two fragments sends $a \to -a$ but cannot change the physical partition, so $Q(a) = Q(-a)$. Expanding both terms about $A/2$ makes the required cancellation explicit:

$$F(A/2 \pm a) = F(A/2) \pm F'(A/2)a + \frac{1}{2}F''(A/2)a^2 \pm \frac{1}{6}F'''(A/2)a^3 + \cdots, \tag{1.15}$$

$$Q(a) = Q(0) + F''(A/2)a^2 + \mathcal{O}(a^4). \tag{1.16}$$

There can be no fixed-δ term linear in a: such a term would assign different Q-values to the same unordered fragment pair merely because its labels were exchanged.

Symmetric estimate. Approximating the parent and symmetric fragments by $b_{\mathrm{p}} = E_0$ and $b(A/2) = E_1$ gives

$$Q(0) = (E_1 - E_0)A. \tag{1.17}$$

With $E_0 \approx 7.6\,\mathrm{MeV}$, $E_1 \approx 8.5\,\mathrm{MeV}$, and $A \approx 240$,

$$Q_{\mathrm{sym}} \approx 0.9 \times 240 = 216\,\mathrm{MeV}. \tag{1.18}$$

Asymmetric case ($a \neq 0$). The sign of $F''(A/2)$, not an arbitrarily fixed slope offset, determines the local liquid-drop curvature. Moreover, pairing, prompt-neutron multiplicity, and fragment shell corrections all vary with partition, so the Taylor model does not predict the full measured $Q(A)$. Nature prefers asymmetric low-energy fission because shell-corrected potential-energy valleys and level densities favour those paths, while Q remains near 200 MeV [6, 1, 14].

Key idea

$Q(a) = Q(-a)$ because fragment labels are interchangeable. Hence the local expansion begins with a^2: $Q(a) = Q(0) + F''(A/2)a^2 + \mathcal{O}(a^4)$. Shell effects, rather than a symmetry-invalid linear term, drive the observed asymmetric yield.

1.5 Prompt neutrons, delayed neutrons, and β chains

1.5.1 Why neutrons are emitted

Heavy nuclei are neutron-rich: for ^{236}U,

$$\frac{N}{Z} = \frac{144}{92} \approx 1.57. \tag{1.19}$$

Stable medium-mass nuclei have smaller N/Z (closer to 1.3–1.4). Immediately after scission the fragments are still neutron-rich and highly excited; they evaporate **prompt neutrons** on a timescale $\lesssim 10^{-14}$ s. For ^{235}U, the ENDF/B-VIII.0 evaluation at $E_n = 0.0253\,\mathrm{eV}$ tabulates total, delayed, and prompt average multiplicities in MF=1, MT=452, 455, and 456, respectively. At thermal energy $\bar{\nu}_{\text{total}} \simeq 2.4355$; subtracting the evaluated delayed component gives approximately

$$\langle \nu_{\text{prompt}} \rangle \approx 2.42. \tag{1.20}$$

The quoted digits identify the evaluation and should not be read as a newly derived experimental uncertainty [35].

1.5.2 Example N/Z after a typical split

For $^{140}\text{Xe} + {}^{94}\text{Sr} + 2n$:

$$\left.\frac{N}{Z}\right|_{\text{Xe}} = \frac{86}{54} \approx 1.59, \qquad \left.\frac{N}{Z}\right|_{\text{Sr}} = \frac{56}{38} \approx 1.47. \tag{1.21}$$

Both fragments remain above the β-stability line after prompt neutron emission.

1.5.3 Beta-decay chains

Neutron-rich fragments decay by successive β^- transitions,

$$n \to p + e^- + \bar{\nu}_e, \tag{1.22}$$

until they reach a stable N/Z. Examples:

$$^{140}\text{Xe} \xrightarrow{\beta^-} {}^{140}\text{Cs} \xrightarrow{\beta^-} {}^{140}\text{Ba} \xrightarrow{\beta^-} {}^{140}\text{La} \xrightarrow{\beta^-} {}^{140}\text{Ce (stable)}, \tag{1.23}$$

$$^{94}\text{Sr} \xrightarrow{\beta^-} {}^{94}\text{Y} \xrightarrow{\beta^-} {}^{94}\text{Zr (stable)}. \tag{1.24}$$

1.5.4 Delayed neutrons

Some β daughters are still neutron-unstable and emit a neutron after a β delay of seconds to minutes. Classic example:

$$^{137}\text{I} \xrightarrow{\beta^-} {}^{137}\text{Xe}^* \to {}^{136}\text{Xe} + n \quad \text{(delayed neutron)}. \tag{1.25}$$

The average number of delayed neutrons per fission is only $\langle \nu_d \rangle \sim 0.016$, giving the *physical yield fraction* $\beta = \bar{\nu}_d/\bar{\nu}_{\text{total}} \simeq 0.0065$. Reactor kinetics instead uses the *effective delayed-neutron fraction* β_{eff}, which weights delayed and prompt neutrons by their different spectra, locations, and importance for sustaining the chain. Thus β_{eff} need not equal β. Delayed-neutron precursor half-lives introduce seconds-to-minutes timescales instead of prompt-generation times of order 10^{-4} s or less [6, 1, 2].

1.5.5 Prompt and delayed gamma rays

Fragments are born excited and emit **prompt γ rays** on the same fast timescale as prompt neutrons. Subsequent β daughters also radiate **delayed γ rays** as they de-excite.

1.6 Energy partition in fission

A typical total energy release of order 200 MeV per fission of ^{236}U is shared approximately as follows [6, 1]:

Channel	Energy (approx.)
Kinetic energy of fission fragments	167 MeV
Kinetic energy of prompt neutrons	5 MeV
Prompt γ rays	6 MeV
β particles from products	8 MeV
Delayed γ rays	7 MeV
Antineutrinos (β decays)	12 MeV

The bulk of the recoverable heat is the kinetic energy of the two fragments (Coulomb repulsion after scission), thermalised in the fuel. Antineutrinos escape and do not heat the reactor. The entries sum to about 205 MeV; delayed-neutron kinetic energy is negligible on this scale. Values are the rounded ^{236}U partition tabulated by Dunlap; evaluated-library totals depend on the precise definition (for example, whether later neutron-capture γ heating is included).

Remark

The fragment kinetic energies are nearly equal in the centre-of-mass frame for equal-mass splits; for asymmetric splits the light fragment carries more kinetic energy (same momentum, smaller mass).

1.7 Cross sections, barrier penetration, and chain reactions

1.7.1 Energy dependence of the fission cross section

Below the barrier, fission proceeds by tunneling; the cross section is exponentially small. As the compound excitation approaches and then exceeds E_f, the effective barrier thins and σ_f rises steeply, then saturates when the process is classically allowed. Resonances and intermediate structure appear when discrete compound states couple to the fission channels. For fissile nuclei, σ_f is huge at thermal energies ($\propto 1/v$ capture into a dense compound spectrum already above E_f); for ^{238}U, σ_f is small until $K_n \sim 1\,\text{MeV}$ [6, 1].

1.7.2 Generations and multiplication

Each fission emits $\langle \nu \rangle \sim 2.4$ neutrons. If, on average, one or more of those neutrons induces another fission, a **chain reaction** results. A generation begins with the neutrons born from one set of fissions and ends when they are absorbed or leak. Define

$$k \equiv \frac{N_{g+1}}{N_g} = \bar{\nu}\, p_{\text{next}}, \qquad N_g = N_0 k^g, \tag{1.26}$$

where p_{next} is the net probability that a source neutron survives leakage and non-fission absorption and produces a next-generation fission:

- $k < 1$: subcritical (dies out);
- $k = 1$: critical (steady power);
- $k > 1$: supercritical (power rises).

In a thermal reactor, fast fission neutrons are slowed by a moderator (water, graphite, ...) to exploit the large thermal σ_f of ^{235}U; heat is removed continuously, engineered feedbacks and absorbers hold $k_{\rm eff} \simeq 1$, and delayed neutrons permit regulation. Writing reactivity as $\rho = (k_{\rm eff} - 1)/k_{\rm eff}$, exact prompt criticality occurs at $\rho = \beta_{\rm eff}$, equivalently

$$k_{\rm eff} = \frac{1}{1 - \beta_{\rm eff}}, \qquad k_{\rm prompt} \equiv k_{\rm eff}(1 - \beta_{\rm eff}) = 1. \tag{1.27}$$

The often quoted $k_{\rm eff} \simeq 1 + \beta_{\rm eff}$ is only the first-order approximation for $\beta_{\rm eff} \ll 1$. An explosive assembly instead undergoes a brief prompt-supercritical excursion with no steady heat-removal or control objective. This distinction is about kinetics and engineering purpose, not a different nuclear reaction; no design details are needed here. Detailed reactor physics (four-factor formula, moderation, poisoning) lies beyond this chapter; the nuclear ingredients are the large thermal σ_f of fissile isotopes, $\langle \nu \rangle > 1$, and the existence of delayed neutrons [6, 1, 14].

Takeaway

- $n + {}^{235}$U: $Q \sim 6.6\,\text{MeV} > E_f \sim 6.2\,\text{MeV}$ (fissile). $n + {}^{238}$U: $Q \sim 4.8\,\text{MeV} < E_f$ (needs $K_n \gtrsim 1\,\text{MeV}$).
- Mass yields: asymmetric peaks near $A \sim 95, 140$; liquid drop alone insufficient.
- Fragment exchange requires $Q(a) = Q(-a)$, so its local asymmetry expansion begins at a^2; the total release is $\sim 200\,\text{MeV}$, mostly fragment KE.
- $\langle \nu \rangle_{\rm total} = 2.4355$ for thermal ^{235}U fission; delayed neutrons are only $\sim 0.65\%$; β is a yield fraction whereas $\beta_{\rm eff}$ is importance weighted.
- $N_g = N_0 k^g$: subcritical, critical, and supercritical correspond to $k < 1$, $k = 1$, and $k > 1$; delayed neutrons enable reactor control.

1.8 Deeper physics: asymmetric fission yields and chain-reaction scale

1.8.1 Asymmetric mass yields

Thermal-neutron fission of ^{235}U produces two heavy fragments with a characteristic **asymmetric** mass distribution: yield peaks near $A \approx 95$ and $A \approx 140$, not at symmetric split $A \approx 117$ [6, 1]. The liquid drop favours symmetric fission near the saddle, but shell corrections stabilise fragments near closed proton and neutron shells ($Z \approx 38$, 50 and $N \approx 82$). The yield curve is therefore a probe of microscopic shell structure, not only of the average Q-value release [14, 54].

Energy release in $^{235}\mathrm{U}(n, f)$

Each fission releases about 200 MeV [1, 35]: roughly 170 MeV in fragment kinetic energy, ~ 30 MeV in prompt γ and neutron emission, with delayed energy from β decay of the fragments over minutes to years. The average prompt neutron multiplicity is $\bar{\nu} \approx 2.4$ for thermal neutrons [6, 35]. Those neutrons, moderated in a reactor, can induce further fissions in fissile material.

1.8.2 Chain reaction and k_{eff}

In a multiplying assembly, each fission generation produces on average k_{eff} fissions in the next generation. Steady operation requires $k_{\mathrm{eff}} \approx 1$. If each fission produces $\bar{\nu}$ neutrons and a fraction p survives to cause another fission,

$$k_{\mathrm{eff}} \approx \bar{\nu}\, p. \tag{1.28}$$

Delayed neutrons ($\sim 0.65\%$ of $\bar{\nu}$ for $^{235}\mathrm{U}$) arrive on second time scales and allow control by rods; prompt neutrons alone would make reactors uncontrollable [6, 1]. The scale separation between prompt ($\sim 10^{-14}$ s) and delayed ($\sim$ 1–100 s) neutron groups is what makes a thermal reactor an engineering possibility rather than an instantaneous energy burst [14].

Key idea

From fission yields to fusion fuel cycles. Fission releases ~ 200 MeV per heavy nucleus; fusion of light nuclei (Lectures 25–26) releases energy by moving up the same binding curve from the opposite direction. Both processes rely on the Q-value and barrier physics developed in the decay and reaction chapters [6, 2].

1.8.3 Pairing and the fissile isotope pattern

The large thermal-neutron fission cross section of $^{235}\mathrm{U}$ and the small capture cross section leading to fission in $^{238}\mathrm{U}$ reflect pairing as well as barrier height [6, 1]. Adding a neutron to odd-A $^{235}\mathrm{U}$ forms even–even $^{236}\mathrm{U}$ with extra pairing binding, increasing S_n and the capture Q. The same pattern makes $^{239}\mathrm{Pu}$ and $^{233}\mathrm{U}$ fissile. Asymmetric yields then reflect shell-stabilised fragments, not the average Q alone [35, 14]. Delayed neutrons from β-decaying fission products provide the control time scale that separates reactor operation from prompt criticality [6, 35].

1.8.4 Ternary fission and scission dynamics

Ternary fission emits a third light charged particle at scission at the 10^{-3} level and probes neck dynamics between the main fragments [6, 2]. The total kinetic energy partition and neutron multiplicity depend on how much energy is dissipated before scission, a topic of active microscopic theory [54]. Evaluated fission-product yields from ENDF/B libraries are used in reactor physics, safeguards, and r-process network calculations that terminate heavy-nucleus synthesis paths [35, 46].

Independent versus cumulative yields differ by β-decay feeding. Reactor antineutrino predictions need both fission yields and subsequent β branching ratios (Lectures 18–19). Safeguards applications similarly depend on consistent evaluated libraries, not only on a schematic asymmetric yield cartoon.

Library versus cartoon

After drawing the asymmetric yield cartoon, open an evaluated yield file and compare peak locations. Note how many isobars contribute under each peak once β feeding is included. The cartoon teaches the idea; the library teaches the data culture of reactors and safeguards.

1.9 Further physics from the literature

Pairing and the fissile pattern. The large capture Q of $n + {}^{235}\mathrm{U}$ relative to $n + {}^{238}\mathrm{U}$ is a pairing effect: adding a neutron to odd-A ${}^{235}\mathrm{U}$ produces even–even ${}^{236}\mathrm{U}$ with an extra pairing energy, increasing the neutron separation energy. The same pattern explains fissile ${}^{239}\mathrm{Pu}$ and ${}^{233}\mathrm{U}$ [6, 1, 14].

Ternary fission and light charged particles. Occasionally a third light charged particle (α, ${}^{3}\mathrm{H}$, ...) is emitted at scission (ternary fission), at the 10^{-3} level. It is a probe of the neck dynamics between the two main fragments [6, 2].

Reactor antineutrinos. Each fission leads to several β^- decays and therefore several $\bar{\nu}_e$. Reactor antineutrino spectra are used for oscillation experiments and for remote monitoring of reactor power and fuel evolution [14, 2].

Evaluated nuclear data. Fission yields, $\bar{\nu}(E)$, and cross sections $\sigma_f(E)$ are tabulated in ENDF/B, JEFF, and JENDL libraries and summarised in ENSDF/NuDat for decay properties of individual fragments [35, 20, 21, 33].

Provenance of the checked numbers. The separation energies $S_n({}^{236}\mathrm{U}) = 6.545\,\mathrm{MeV}$ and $S_n({}^{239}\mathrm{U}) = 4.806\,\mathrm{MeV}$ use AME2020 masses through NNDC QCalc [27, 21]. The IAEA Nuclear Data for Safeguards table gives $\bar{\nu}_{\mathrm{total}} = 2.4355 \pm 0.0023$ for thermal-neutron fission of ${}^{235}\mathrm{U}$; the commonly used delayed fraction is about 0.65%. The rounded 205 MeV partition in Section 1.6 follows Dunlap's ${}^{236}\mathrm{U}$ table. These sources define quantities more carefully than the original OCR and explain small differences among values quoted in lecture notes [35, 33].

Connection to the H. C. Verma sequence. NPTEL course 115104043 treats fission basics, uranium fission, and reactors in Lectures 33–35. The present chapter follows that progression but stops at course-safe principles: generations, k_{eff}, moderation, absorbers, feedback, and delayed-neutron control. It does not address assembly design or other engineering details of explosive systems [32].

Reading guide

Krane [6] Ch. 13 (induced fission, yields, reactors); Dunlap [1] (energetics and neutron emission); Basdevant [14] (chain reactions); Demtröder [2] (experimental systematics).

1.9.1 Quantitative asymmetric yield and Q release

The asymmetric fission yield $Y(A)$ integrates to two fragment peaks. The total energy release per event is approximately constant (~ 200 MeV), but the partition between fragment kinetic energy, prompt neutrons, and γ rays depends on the mass split [1, 35]. Light fragments carry higher kinetic energy per nucleon because Coulomb repulsion accelerates them from a compact scission configuration. Delayed energy from fragment β decay adds ~ 10 MeV per fission over minutes to years, relevant for reactor decay-heat calculations [6, 35].

Neutron multiplication scale in a thermal reactor

Thermal fission of ^{235}U emits $\bar{\nu} \approx 2.44$ prompt neutrons [35]. In an infinite medium with fission cross section $\sigma_f \approx 585$ b and number density $n \approx 0.05\,\mathrm{fm}^{-3}$, the mean free path is $\lambda_f = 1/(n\sigma_f) \approx 34$ cm. If fraction $p \approx 0.4$ of neutrons cause another fission after moderation, $k_{\mathrm{eff}} \approx \bar{\nu}p \approx 1$ for critical operation (1.28) [6, 14]. Delayed neutrons stretch the generation time from nanoseconds to seconds, enabling control.

1.9.2 From fission chains to fusion fuel cycles

Fission releases ~ 200 MeV per heavy nucleus; D–T fusion releases ~ 17.6 MeV per event but with far higher specific energy per nucleon transferred to light products [1, 6]. Both processes move toward the iron peak on the binding-energy curve: fission from above, fusion from below (Lectures 25–26). Reactor antineutrinos from fragment β chains connect fission to the weak-interaction spectroscopy of Lectures 18–19 [14, 2]. r-process recycling through fission in neutron-star mergers uses the same yield libraries as reactor safeguards [46, 54].

Key idea

Arc through the course. Asymmetric yields (Lecture 24) reflect shell corrections to the fission saddle (Lecture 23). Chain-reaction scale sets reactor engineering; fusion reactivity $\langle\sigma v\rangle$ sets stellar lifetimes (Lecture 26). Both require barrier penetration developed in Lectures 16–17 and 25 [6, 36].

1.9.3 Decay heat and the β-γ cascade after fission

Prompt fission releases ~ 200 MeV in fragments, neutrons, and γ rays; delayed energy from fragment β decay adds ~ 7 MeV per fission on a ~ 10 min scale and continues for years [1, 35]. Each β step is a continuous spectrum (Lecture 18) followed by γ cascades governed by multipole rules (Lecture 20) [6]. Reactor safety calculations require cumulative fission yields and decay-heat tables that are consistent with independent β branch data [35, 33]. The same fragment β chains produce reactor antineutrinos used in oscillation experiments [14, 2].

1.10 Deeper reading: yields, delayed neutrons, and r-process recycling

Asymmetric mass yields for thermal $^{235}\mathrm{U}(n, f)$ reflect shell stabilisation of fragments near $A \sim 95$ and $A \sim 140$. Symmetric yields appear at higher excitation energy. Delayed-neutron precursors control reactor timescales on the order of seconds; cumulative yields enter decay-heat and safeguards calculations.

In neutron-star merger ejecta, fission recycling terminates the r-process path beyond $A \sim 195$ and reshapes abundances. Microscopic yield models for exotic actinides remain uncertain compared with evaluated libraries for major actinides. The lecture chain-reaction discussion is the reactor face of the same nuclear data.

Energy dependence of yields

As excitation energy rises, shell-stabilised asymmetric valleys fill in and symmetric fission becomes more competitive. Multichance fission (neutron emission before fission) further complicates yield interpretation in hot heavy-ion reactions. Reactor applications mostly need thermal and fast-neutron libraries; astrophysics needs far-off-stability estimates.

Delayed neutrons and control

Groups of delayed-neutron precursors with different half-lives create the effective β_{eff} that makes reactors controllable. Connecting those groups to β-delayed neutron branching ratios from Lecture 18 closes the nuclear-data loop.

Yield and reactor drill

Using a published thermal yield table for $^{235}\mathrm{U}$, identify the light and heavy peak mass numbers and estimate the peak-to-valley ratio. Then list three delayed-neutron precursor isotopes and their half-life groups. Connect each precursor to a β-delayed neutron branch (Lecture 18).

Write a short paragraph on r-process fission recycling: where the path hits fission, fragments return to lower A and capture again, smoothing abundance patterns above $A \sim 195$. Emphasise that exotic actinide yields are much less constrained than reactor actinides, so astrophysical abundance predictions inherit nuclear-data uncertainties from this chapter's themes.

Yields connect nuclear structure to reactors and to r-process recycling. Evaluated libraries are the data backbone behind the asymmetric-yield cartoon.

In practice, rework one numerical estimate from the lecture with a different parameter set and compare the shift to the quoted experimental uncertainty. If the shift exceeds the uncertainty, the estimate is teaching a scale, not delivering a fit. That distinction keeps theoretical cartoons honest when they sit beside evaluated data tables and modern many-body calculations. Along the course arc, write one sentence linking this chapter backward and one forward: the discipline of those two sentences is as important as any single formula. Examination problems rarely ask for a literature review, but they do ask for the scale argument that literature reviews presuppose.

Synthesis problem

Write a half-page note that (i) restates the chapter's central scale or selection rule in one equation, (ii) evaluates it numerically for one concrete nucleus or energy, and (iii) names the neighbouring lecture that uses the result. Keep the note free of research-frontier speculation; the goal is fluency with the lecture physics itself. If an assumption fails (Born approximation, spherical mean field, allowed transition, one-dimensional barrier), state the failure mode in a final sentence. That habit converts passive reading into examination-ready understanding and makes the later research-frontier box read as an extension rather than a replacement.

Research frontier: fission yields, reactors, and r-process recycling

Mass-yield curves and chain-reaction ideas of Lecture 24 connect directly to evaluated fission-product libraries used in reactors and safeguards [35]. Astrophysically, fission recycling shapes the abundance pattern beyond $A \sim 195$ in neutron-star merger ejecta; yield models and β-delayed fission remain major uncertainties in r-process simulations [46, 51, 54]. Microscopic yield predictions are beginning to replace purely empirical systematics for exotic actinides, but they must still be validated against radiochemical and on-line mass-spectrometric data. Reactor applications add a second demand: delayed-neutron precursors and cumulative yields control reactivity and safeguards signatures. Open research questions include the energy dependence of yields for exotic fissioning systems and the coupling between fission and β-decay networks in merger outflows.

For safeguards and reactor modelling, cumulative and independent yields, decay heat, and delayed-neutron fractions must be consistent within evaluated libraries. Students who compare two library releases for the same fissioning system quickly see where nuclear data, not just reactor engineering, set the uncertainty budget.

Comparing two evaluated-library releases for the same fissioning system quickly reveals where nuclear data dominate the uncertainty budget.

That data-driven uncertainty view links the lecture yield curve to real reactor and astrophysics applications.

Student directions. (1) Data exercise: using an ENDF fission-yield table, identify the two asymmetric peaks for thermal $^{235}\mathrm{U}(n, f)$. (2) Reactor estimate: estimate the number of delayed-neutron precursors that matter for reactor control on the $\sim 10\,\mathrm{s}$ scale. (3) Short essay: explain how fission terminates the r-process path and which nuclear data are most urgently needed.

1.11 Problems with solutions

Problem 24.1 — Fissile vs fissionable

Given $Q(n + {}^{235}\mathrm{U}) = 6.55\,\mathrm{MeV}$, $E_f({}^{236}\mathrm{U}) = 6.2\,\mathrm{MeV}$, $Q(n + {}^{238}\mathrm{U}) = 4.80\,\mathrm{MeV}$, and $E_f({}^{239}\mathrm{U}) = 6.2\,\mathrm{MeV}$, determine for each case whether thermal neutrons can induce fission, and estimate the neutron kinetic energy threshold for $^{238}\mathrm{U}$ [6, 1].

Solution 24.1

Step 1 (^{235}U). Excitation $E^* \approx 6.55\,\text{MeV} > 6.2\,\text{MeV}$. Thermal neutrons induce fission: fissile.

Step 2 (^{238}U). $E^* \approx 4.80\,\text{MeV} < 6.2\,\text{MeV}$. Thermal fission is blocked by a residual barrier $\approx 1.4\,\text{MeV}$.

Step 3 (threshold). Need $Q + K_n \gtrsim E_f$, so

$$K_n \gtrsim 6.2 - 4.8 = 1.4\,\text{MeV}.$$

(Laboratory thresholds are of this order; precise values include CM corrections and barrier tunneling tails.)

Problem 24.2 — Exchange-symmetric asymmetry expansion

Let $F(x)$ be the total binding of a fragment of mass x, so $Q(a) = F(120-a)+F(120+a)-B_\text{p}$ for a parent with $A = 240$. Show that all odd powers of a cancel. If $Q(0) = 216\,\text{MeV}$ and $F''(120) = -5.0 \times 10^{-3}\,\text{MeV}$, estimate $Q(20)$ through quadratic order and verify that $a = 20$ and $a = -20$ give the same result.

Solution 24.2

Step 1: expand both fragment bindings.

$$F(120 \pm a) = F(120) \pm F'(120)a + \frac{1}{2}F''(120)a^2 \pm \frac{1}{6}F'''(120)a^3 + \cdots .$$

Adding the two expansions cancels the linear, cubic, and all other odd terms:

$$Q(a) = Q(0) + F''(120)a^2 + \mathcal{O}(a^4) = Q(-a).$$

Step 2: evaluate the toy curvature.

$$Q(\pm 20) = 216 + (-5.0 \times 10^{-3})(20)^2 = 214\,\text{MeV}.$$

The chosen negative curvature lowers the toy-model Q by $2\,\text{MeV}$, but the sign and magnitude of the actual partition dependence require masses, prompt-neutron channels, and shell corrections [6, 14].

Problem 24.3 — Neutrons from N/Z

^{236}U has $Z = 92$, $N = 144$. Suppose it splits into fragments with $Z_1 = 54$, $Z_2 = 38$ without emitting neutrons, sharing N in proportion to A. Argue why prompt neutron emission is expected, given that stable $A \sim 90$–140 nuclei have $N/Z \sim 1.3$–1.4.

Solution 24.3

Step 1. Parent $N/Z = 144/92 \approx 1.57$.

Step 2. Conserving N/Z in each fragment leaves both with $N/Z \sim 1.57$, far above the stable valley at those Z.

Step 3. Excess neutrons are weakly bound in the hot fragments and evaporate as prompt neutrons until the neutron separation energy rises. Residual neutron richness is then removed slowly by β^- decay [1, 6].

Problem 24.4 — Energy partition

If 200 MeV is released per fission and 160 MeV appears as fragment kinetic energy, what fraction of the energy is carried by fragments? If a reactor fissions 10^{19} nuclei per second, estimate the fragment-heating power in megawatts.

Solution 24.4

Step 1. Fraction: $160/200 = 0.80$ (80%).

Step 2. Energy per second from fragments:

$$P = 10^{19} \times 160\,\mathrm{MeV/s}.$$

Convert: $1\,\mathrm{MeV} = 1.602 \times 10^{-13}\,\mathrm{J}$, so

$$P = 10^{19} \times 160 \times 1.602 \times 10^{-13}\,\mathrm{W} \approx 2.56 \times 10^{8}\,\mathrm{W} \approx 256\,\mathrm{MW}.$$

(Total thermal power including other channels would be $\sim 320\,\mathrm{MW}$ before neutrino losses.)

Problem 24.5 — Multiplication factor and generations

In a certain assembly, each fission produces on average 2.4 neutrons, and the probability that a neutron induces another fission (rather than leaking or being captured non-fissilely) is $p = 0.40$. Find k, classify the assembly, and find N_{10}/N_0. Repeat the generation calculation for $p = 0.425$.

Solution 24.5

$$k = \langle \nu \rangle\, p = 2.4 \times 0.40 = 0.96 < 1.$$

The assembly is subcritical: the chain dies out. Raising enrichment, reducing leakage, or improving moderation can increase p until $k = 1$ [6, 1].

Step 2.

$$\frac{N_{10}}{N_0} = k^{10} = 0.96^{10} = 0.665.$$

After ten generations about two-thirds of the original generation remains on average.

Step 3. If $p = 0.425$, then $k = 2.4(0.425) = 1.02$, and

$$\frac{N_{10}}{N_0} = 1.02^{10} = 1.219.$$

The same exponential law distinguishes a slowly decaying subcritical chain from a growing supercritical one; it does not by itself specify the elapsed time, which also requires the generation lifetime.

Problem 24.6 — Delayed fraction and prompt criticality

Suppose $\langle \nu_{\text{prompt}} \rangle = 2.43$ and $\langle \nu_{\text{delayed}} \rangle = 0.016$. What fraction β of neutrons are delayed? Explain why this yield fraction is not generally β_{eff}. If $\beta_{\text{eff}} = 0.0065$, find the exact prompt-critical k_{eff}.

Solution 24.6

Step 1.

$$\beta = \frac{0.016}{2.43 + 0.016} \approx 0.0065 \quad (0.65\%).$$

Step 2. The physical β counts emitted neutrons. β_{eff} additionally weights their spectra and birth locations by their importance to the chain, so the two quantities need not be equal.

Step 3. Prompt criticality is $\rho = \beta_{\text{eff}}$, where $\rho = (k_{\text{eff}} - 1)/k_{\text{eff}}$. Hence

$$k_{\text{eff,prompt}} = \frac{1}{1 - \beta_{\text{eff}}} = \frac{1}{1 - 0.0065} = 1.00654.$$

The approximation $1 + \beta_{\text{eff}} = 1.0065$ is close but not exact. Below this prompt-critical threshold, delayed-neutron precursor timescales make mechanical control possible [6, 1].

Problem 24.7 — Separation energy and threshold

AME2020 gives $S_n(^{236}\text{U}) = 6.545\,\text{MeV}$ and $S_n(^{239}\text{U}) = 4.806\,\text{MeV}$. Using the original lecture's one-barrier value $E_f = 6.2\,\text{MeV}$, calculate the excess or deficit $E^* - E_f$ after capture of a negligible-energy neutron on ^{235}U and ^{238}U. Why should the second result not be quoted as a precision experimental threshold? [27, 21]

Solution 24.7

Step 1: identify the capture energy. For a target ^{A}U,

$$E^* \simeq S_n(^{A+1}\text{U}) + E_{n,\text{cm}}.$$

For a thermal neutron $E_{n,\text{cm}}$ is negligible on the MeV scale.

Step 2: $^{235}\textbf{U}$**.**

$$E^* - E_f = 6.545 - 6.2 = +0.345\,\text{MeV}.$$

The compound $^{236}\mathrm{U}^*$ is formed above the illustrative barrier.
Step 3: ^{238}U.

$$E^* - E_f = 4.806 - 6.2 = -1.394\,\mathrm{MeV}.$$

Thus a fast-neutron energy of order $1\,\mathrm{MeV}$ is expected before fission becomes strong.
Step 4: limitation. The mass-derived separation energies are precise, but "the barrier" is a double-humped, spin-dependent transmission problem, and tunnelling gives a subthreshold tail. Centre-of-mass kinematics and competing channels also matter. Hence $1.394\,\mathrm{MeV}$ is a model estimate, not a sharp measured threshold.

Bibliography

[1] R. A. Dunlap, *An Introduction to the Physics of Nuclei and Particles* (2nd ed.), IOP Publishing, Bristol (2023), DOI: 10.1088/978-0-7503-6094-4, Ch. 3 (Nuclear composition and size).

[2] W. Demtröder, *Nuclear and Particle Physics*, Undergraduate Lecture Notes in Physics, Springer, Cham (2023).

[3] S. Petrera, *Problems and Solutions in Nuclear and Particle Physics*, UNITEXT for Physics, Springer, Cham (2019).

[4] F. Terranova, *A Modern Primer in Particle and Nuclear Physics*, Oxford University Press (2021).

[5] S. D'Auria, *Introduction to Nuclear and Particle Physics*, Undergraduate Lecture Notes in Physics, Springer, Cham (2018).

[6] K. S. Krane, *Introductory Nuclear Physics*, Wiley, New York (1988).

[7] R. Hofstadter, "Electron scattering and nuclear structure," Rev. Mod. Phys. **28**, 214 (1956).

[8] H. F. Ehrenberg, R. Hofstadter, U. Meyer-Berkhout, D. G. Ravenhall, and S. E. Sobottka, "High-Energy Electron Scattering and the Charge Distribution of Carbon-12 and Oxygen-16," Phys. Rev. **113**, 666 (1959).

[9] H. Yukawa, "On the interaction of elementary particles. I," Proc. Phys.-Math. Soc. Japan **17**, 48 (1935).

[10] R. D. Woods and D. S. Saxon, "Diffuse surface optical model for nucleon-nuclei scattering," Phys. Rev. **95**, 577 (1954).

[11] H. G. J. Moseley, "The high-frequency spectra of the elements," Phil. Mag. **26**, 1024 (1913); **27**, 703 (1914).

[12] C. F. von Weizsäcker, "Zur Theorie der Kernmassen," Z. Phys. **96**, 431 (1935).

[13] P. Cappellaro, *Introduction to Applied Nuclear Physics* (MIT OpenCourseWare / LibreTexts), CC BY-NC-SA 4.0.

[14] J.-L. Basdevant, J. Rich, and M. Spiro, *Fundamentals in Nuclear Physics: From Nuclear Structure to Cosmology*, Springer, New York (2005).

[15] D. Tong, *Particle Physics*, Lecture notes (University of Cambridge / CERN school notes).

[16] M. G. Mayer, "On closed shells in nuclei. II," Phys. Rev. **75**, 1969 (1949).

[17] O. Haxel, J. H. D. Jensen, and H. E. Suess, "On the "magic numbers" in nuclear structure," Phys. Rev. **75**, 1766 (1949).

[18] T. Schmidt, "Über die magnetischen Momente der Atomkerne," Z. Phys. **106**, 358 (1937).

[19] L. W. Nordheim, "On spins, moments, and shells in nuclei," Phys. Rev. **78**, 294 (1950).

[20] Evaluated Nuclear Structure Data File (ENSDF), National Nuclear Data Center, Brookhaven National Laboratory, `https://www.nndc.bnl.gov/ensdf/`.

[21] NuDat 3, National Nuclear Data Center, Brookhaven National Laboratory, `https://www.nndc.bnl.gov/nudat3/`.

[22] N. J. Stone, "Table of nuclear magnetic dipole and electric quadrupole moments," At. Data Nucl. Data Tables **90**, 75 (2005); updated compilations at NNDC.

[23] W. N. Cottingham and D. A. Greenwood, *An Introduction to Nuclear Physics* (2nd ed.), Cambridge University Press, Cambridge (2001).

[24] H. Geiger and J. M. Nuttall, "The ranges of the α particles from the radioactive substances," Phil. Mag. **22**, 613 (1911).

[25] G. Gamow, "Zur Quantentheorie des Atomkernes," Z. Phys. **51**, 204 (1928).

[26] R. W. Gurney and E. U. Condon, "Wave mechanics and radioactive disintegration," Nature **122**, 439 (1928); Phys. Rev. **33**, 127 (1929).

[27] M. Wang, W. J. Huang, F. G. Kondev, G. Audi, and S. Naimi, "The AME 2020 atomic mass evaluation (II). Tables, graphs and references," Chin. Phys. C **45**, 030003 (2021).

[28] Laboratoire National Henri Becquerel (LNHB), Recommended decay data, `http://www.lnhb.fr/nuclear-data/nuclear-data-table/`.

[29] L. M. Langer, R. D. Moffat, and H. C. Price, Jr., "Low energy beta-ray spectra: P^{32} and Cu^{64}," Phys. Rev. **76**, 1725 (1949).

[30] L. M. Langer and H. C. Price, Jr., "Shapes of the beta-spectra of the forbidden transitions of Sb^{124}, Rb^{86}, Sr^{89}, Y^{91}, and Cs^{137}," Phys. Rev. **75**, 1769 (1949).

[31] D. C. Camp and L. M. Langer, "The shape of the ^{66}Ga positron spectrum and the contribution from $0^+ \to 0^+$ transitions," Phys. Rev. **129**, 1782 (1963).

[32] H. C. Verma, *Nuclear Physics: Fundamentals and Applications*, NPTEL/IIT Kanpur lecture series, `https://hcverma.in/ncl_phy_lectures`.

[33] International Atomic Energy Agency, *LiveChart of Nuclides*, evaluated structure, decay, reaction, and fission-yield data, `https://www-nds.iaea.org/relnsd/vcharthtml/VChartHTML.html`.

[34] T. Kibédi, T. W. Burrows, M. B. Trzhaskovskaya, P. M. Davidson, and C. W. Nestor, Jr., "Evaluation of theoretical conversion coefficients using BrIcc," Nucl. Instrum. Methods Phys. Res. A **589**, 202 (2008), DOI: 10.1016/j.nima.2008.02.051.

[35] D. A. Brown *et al.*, "ENDF/B-VIII.0: The 8th major release of the nuclear reaction data library with CIELO-project cross sections, new standards and thermal scattering data," Nucl. Data Sheets **148**, 1 (2018), DOI: 10.1016/j.nds.2018.02.001.

[36] B. Acharya *et al.*, "Solar fusion III: New data and theory for hydrogen-burning stars," Rev. Mod. Phys. **97**, 035002 (2025), DOI: 10.1103/8lm7-gs18.

[37] S. N. Ghoshal, "An experimental verification of the theory of compound nucleus," Phys. Rev. **80**, 939 (1950), DOI: 10.1103/PhysRev.80.939.

[38] D. Adhikari *et al.* (PREX Collaboration), "Accurate determination of the neutron skin thickness of ^{208}Pb through parity-violation in electron scattering," Phys. Rev. Lett. **126**, 172502 (2021), DOI: 10.1103/PhysRevLett.126.172502.

[39] B. T. Reed, F. J. Fattoyev, C. J. Horowitz, and J. Piekarewicz, "Implications of PREX-II on the equation of state of neutron-rich matter," Phys. Rev. Lett. **126**, 172503 (2021), DOI: 10.1103/PhysRevLett.126.172503.

[40] B. Hu *et al.*, "Ab initio predictions link the neutron skin of ^{208}Pb to nuclear forces," Nature Phys. **18**, 1196 (2022), DOI: 10.1038/s41567-022-01715-8.

[41] E. Epelbaum, H.-W. Hammer, and U.-G. Meißner, "Modern theory of nuclear forces," Rev. Mod. Phys. **81**, 1773 (2009), DOI: 10.1103/RevModPhys.81.1773.

[42] H.-W. Hammer, S. König, and U. van Kolck, "Nuclear effective field theory: Status and perspectives," Rev. Mod. Phys. **92**, 025004 (2020), DOI: 10.1103/RevModPhys.92.025004.

[43] T. Otsuka, A. Gade, O. Sorlin, T. Suzuki, and Y. Utsuno, "Evolution of shell structure in exotic nuclei," Rev. Mod. Phys. **92**, 015002 (2020), DOI: 10.1103/RevModPhys.92.015002.

[44] H. Hergert, S. K. Bogner, T. D. Morris, A. Schwenk, and K. Tsukiyama, "The in-medium similarity renormalization group: A novel ab initio method for nuclei," Phys. Rep. **621**, 165 (2016), DOI: 10.1016/j.physrep.2015.12.007.

[45] J. M. Lattimer and M. Prakash, "The equation of state of hot, dense matter and neutron stars," Phys. Rep. **621**, 127 (2016), DOI: 10.1016/j.physrep.2015.12.005.

[46] J. M. Lattimer, "Neutron stars and the nuclear matter equation of state," Annu. Rev. Nucl. Part. Sci. **71**, 433 (2021), DOI: 10.1146/annurev-nucl-102419-124827.

[47] B. P. Abbott *et al.* (LIGO Scientific Collaboration and Virgo Collaboration), "GW170817: Observation of gravitational waves from a binary neutron star inspiral," Phys. Rev. Lett. **119**, 161101 (2017), DOI: 10.1103/PhysRevLett.119.161101.

[48] M. J. Dolinski, A. W. P. Poon, and W. Rodejohann, "Neutrinoless double-beta decay: Status and prospects," Annu. Rev. Nucl. Part. Sci. **69**, 219 (2019), DOI: 10.1146/annurev-nucl-101918-023407.

[49] M. Agostini, G. Benato, J. A. Detwiler, J. Menéndez, and F. Vissani, "Toward the discovery of matter creation with neutrinoless $\beta\beta$ decay," Rev. Mod. Phys. **95**, 025002 (2023), DOI: 10.1103/RevModPhys.95.025002.

[50] P. Gysbers *et al.*, "Discrepancy between experimental and theoretical β-decay rates resolved from first principles," Nature Phys. **15**, 428 (2019), DOI: 10.1038/s41567-019-0450-7.

[51] H. L. Crawford, K. Fossez, S. König, and A. Spyrou, "A vision for the science of rare isotopes," Annu. Rev. Nucl. Part. Sci. **74**, 141 (2024), DOI: 10.1146/annurev-nucl-121423-091501.

[52] Nuclear Science Advisory Committee, *A New Era of Discovery: The 2023 Long Range Plan for Nuclear Science*, U.S. Department of Energy and National Science Foundation (2023), `https://nuclearsciencefuture.org/`.

[53] S. A. Giuliani, Z. Matheson, W. Nazarewicz, E. Olsen, P.-G. Reinhard, J. Sadhukhan, B. Schuetrumpf, N. Schunck, and P. Schwerdtfeger, "Colloquium: Superheavy elements: Oganesson and beyond," Rev. Mod. Phys. **91**, 011001 (2019), DOI: 10.1103/RevModPhys.91.011001.

[54] N. Schunck and D. Regnier, "Theory of nuclear fission," Prog. Part. Nucl. Phys. **125**, 103963 (2022), DOI: 10.1016/j.ppnp.2022.103963.

[55] I. Counts, J. Hur, D. P. L. Aude Craik, H. Jeon, C. Leung, J. C. Berengut, A. Geddes, A. Kawasaki, W. Jhe, and V. Vuletić, "Evidence for nonlinear isotope shift in Yb^+ search for new boson," Phys. Rev. Lett. **125**, 123002 (2020), DOI: 10.1103/PhysRevLett.125.123002.

[56] I. Angeli and K. P. Marinova, "Table of experimental nuclear ground state charge radii: An update," At. Data Nucl. Data Tables **99**, 69 (2013), DOI: 10.1016/j.adt.2011.12.006.

[57] S. Kraemer *et al.*, "Observation of the radiative decay of the ^{229}Th nuclear clock isomer," Nature **617**, 706 (2023), DOI: 10.1038/s41586-023-05894-z.